Received: 27 July 2021 | Revised: 19 September 2021 | Accepted: 25 September 2021

DOI: 10.1002/jnr.24980

RESEARCH ARTICLE

JOURNAL OF Neuroscience Research

Increased susceptibility to quinolinic acid-induced seizures and long-term changes in brain oscillations in an animal model of glutaric acidemia type I

Letícia Barbieri Caus[1,2] | Mayara Vendramin Pasquetti[1] | Bianca Seminotti[3] | Michael Woontner[4] | Moacir Wajner[3] | Maria Elisa Calcagnotto[1,2,3]

[1]Neurophysiology and Neurochemistry of Neuronal Excitability and Synaptic Plasticity Laboratory (NNNESP Lab), Biochemistry Department, Universidade Federal do Rio Grande do Sul, Porto Alegre, Brazil

[2]Graduate Program in Neuroscience, ICBS, Universidade Federal do Rio Grande do Sul, Porto Alegre, Brazil

[3]Graduate Program in Biological Sciences: Biochemistry, Department of Biochemistry, Universidade Federal do Rio Grande do Sul, Porto Alegre, Brazil

[4]Department of Pediatrics, University of Colorado Denver, Aurora, Colorado, USA

Correspondence
Maria Elisa Calcagnotto, Neurophysiology and Neurochemistry of Neuronal Excitability and Synaptic Plasticity Laboratory (NNNESP Lab), Biochemistry Department, ICBS, Universidade Federal do Rio Grande do Sul (UFRGS), Rua Ramiro Barcelos, 2600, Annex 21111, 90035-003, Porto Alegre, RS, Brazil.
Email: elisa.calcagnotto@ufrgs.br

Funding information
This work was supported by Conselho Nacional de Desenvolvimento Científico e Tecnológico (CNPq), Brazil [grant number 465671/2014-4] and Coordenação de Aperfeiçoamento de Pessoal de Nível Superior (CAPES).

Abstract

Glutaric acidemia type I (GA-I) is an inborn error of metabolism of lysine, hydroxylysine, and tryptophan, caused by glutaryl-CoA-dehydrogenase (GCDH) deficiency, characterized by the buildup of toxic organic acids predominantly in the brain. After acute catabolic states, patients usually develop striatal degeneration, but the mechanisms behind this damage are still unknown. Quinolinic acid (QA), a metabolite of the kynurenine pathway, increases especially during infections/inflammatory processes, and could act synergically with organic acids, contributing to the neurological features of GA-I. The aim of this study was to investigate whether QA increases seizure susceptibility and modifies brain oscillation patterns in an animal model of GA-I, the *Gcdh*$^{-/-}$ mice taking high-lysine diet (*Gcdh*$^{-/-}$-Lys). Therefore, the characteristics of QA-induced seizures and changes in brain oscillatory patterns were evaluated by video-electroencephalography (EEG) analysis recorded in *Gcdh*$^{-/-}$-Lys, *Gcdh*$^{+/+}$-Lys, and *Gcdh*$^{-/-}$-N (normal diet) animals. We found that the number of seizures *per* animal was similar for all groups receiving QA, *Gcdh*$^{-/-}$-Lys-QA, *Gcdh*$^{+/+}$-Lys-QA, and *Gcdh*$^{-/-}$-N-QA. However, severe seizures were observed in the majority of *Gcdh*$^{-/-}$-Lys-QA mice (82%), and only in 25% of *Gcdh*$^{+/+}$-Lys-QA and 44% of *Gcdh*$^{-/-}$-N-QA mice. All *Gcdh*$^{-/-}$-Lys animals developed spontaneous recurrent seizures (SRS), but *Gcdh*$^{-/-}$-Lys-QA animals had increased number of SRS, higher mortality rate, and significant predominance of lower frequency oscillations on EEG. Our results suggest that QA plays an important role in the neurological features of GA-I, as *Gcdh*$^{-/-}$-Lys mice exhibit increased susceptibility to intrastriatal QA-induced seizures and long-term changes in brain oscillations.

KEYWORDS

brain oscillations, electroencephalogram, glutaric acidemia type I, quinolinic acid, seizures, striatum

Edited by Carlos Cepeda and Junie Warrington. Reviewed by Abel Santamaria.

1 | INTRODUCTION

Glutaric acidemia type I (GA-I) is an intoxicating inborn error of amino acid metabolism, caused by the deficiency of glutaryl-CoA-dehydrogenase (GCDH) (Koeller et al., 2002). This mitochondrial enzyme participates in lysine, hydroxylysine, and tryptophan catabolism. GCDH activity deficiency leads to a buildup of organic acids, such as glutaric, 3-hydroxyglutaric, and glutaconic acids, and glutarylcarnitine in body fluids and tissues, chiefly in the brain (Kölker et al., 2011). Patients with GA-I present mainly neurological signs and symptoms, including frontotemporal atrophy, striatal degeneration, progressive dystonia, intellectual impairment, and epilepsy as consequences of acute catabolic states usually triggered by infections and leading to episodes of acute encephalopathy (Goodman, 2004; Lindner et al., 2004; Wajner, 2019), during which the striatum appears to be particularly vulnerable (Amaral et al., 2019; Wajner, 2019). Early diagnosis and treatment based on a low-lysine diet are essential for good neurological outcome. However, early diagnosis can be complicated by the nonspecificity of organic acidemias' symptomatology and poor adherence to therapy can worsen the prognosis (Boy et al., 2021; Wajner, 2019).

Koeller et al. (2002) developed a murine model of GA-I, knocking out the *Gcdh* gene (*Gcdh*$^{-/-}$). *Gcdh*$^{-/-}$ mice were able to replicate the genotype of patients with GA-I, but they lacked some of the main neurological findings of this disease, such as striatal damage (Koeller et al., 2002). This model was further improved by Zinnanti et al. (2006). With high-lysine diet intake, this murine model (*Gcdh*$^{-/-}$-Lys) was able to exhibit many of the common neurological characteristics of GA-I in humans, such as striatal damage, neuronal loss, and spontaneous recurrent seizures (SRS) (Vendramin Pasquetti et al., 2017; Zinnanti et al., 2006), being reliable for GA-I neuropathology studies (Zinnanti et al., 2006).

Since the first report of GCDH deficiency in humans (Goodman et al., 1975), many hypotheses have been postulated to explain the neuropathology of this disease. One of them pinpoints the buildup of quinolinic acid (QA), a metabolite from the kynurenine pathway, the main tryptophan catabolic pathway, in the brain (Heyes, 1987). It has been hypothesized that, during infections, the kynurenine pathway is activated, leading to increased QA concentrations in the brain and subsequently to neurodegeneration in GA-I (Varadkar & Surtees, 2004). QA is known to induce excitotoxicity by acting as an *N*-methyl-D-aspartate (NMDA) receptor agonist (La Cruz et al., 2012), decreasing GABA synthesis and acting synergically with organic acids that accumulate in fluids and tissues of patients with GA-I (Colín-González et al., 2015), causing striatal damage and seizures (Pierozan et al., 2014). Indeed, seizures are commonly observed in patients with GA-I, mainly during episodes of acute encephalopathy (Cerisola et al., 2009; McClelland et al., 2009). Cohort studies show that more than half of patients with GA-I have seizures at early stages (Sitta et al., 2021), which are frequently refractory to available antiepileptic drugs (McClelland et al., 2009).

Qualitative and quantitative analyses of electroencephalogram (EEG) previously published by our group showed that *Gcdh*$^{-/-}$-Lys mice have increased the power of delta and decreased the power of theta and gamma oscillations in the cortex and develop SRS 4 days after high-lysine diet intake (Vendramin Pasquetti et al., 2017). Patients with GA-I also show EEG with bursts of high-amplitude and fast activity and periods of slow background activity (Stigsby et al., 1994; Yalnizoğlu et al., 2005). In addition, EEG analyses have shown that QA induced seizures and increments of power of low-frequency oscillations in other experimental models. Thus, these EEG analyses in *Gcdh*$^{-/-}$-Lys mice after intracerebral QA administration can bring new information concerning QA effects on GA-I neuropathology, as patterns of brain oscillations reflect the activity of distinct neuronal networks and behavioral states and modify in neurological conditions (Buzsáki, 2006). Therefore, here we performed an *in vivo* electrophysiological analysis to evaluate brain oscillation patterns and seizure activity in *Gcdh*$^{-/-}$-Lys mice receiving intrastriatal QA injection to investigate the role of QA in the neurological features in GA-I.

Significance

Glutaric acidemia type I (GA-I) is an inborn error of metabolism characterized by a systemic buildup of organic acids, mainly in the brain. Although activation of kynurenine pathway during acute infections/inflammatory processes increases the metabolite quinolinic acid (QA) in the brain in GA-I, mechanisms behind neurological damage after acute catabolic states in GA-I are still unknown. Here, we showed increased seizure susceptibility, changes in cortical oscillation patterns, and increased mortality rate in animal model of GA-I following QA intrastriatal injection, emphasizing the crucial role of QA in the neurological features in GA-I, particularly in the ictogenesis during infection-induced acute encephalopathy.

2 | MATERIAL AND METHODS

2.1 | Animals

Male and female *Gcdh*$^{+/+}$ and *Gcdh*$^{-/-}$ mice on a 1295vEv background (28–34 days old) were obtained from HCPA Animal Facility. Animals were housed in 22 × 37 × 18 cm acrylic glass cages (up to five animals per cage before surgery and one per cage after surgery) in an acclimatized room (22–26°C) with a 12-hr light/dark cycle. The study design and procedures were reported according to the Animals in Research: Reporting of in Vivo Experiments (ARRIVE) guidelines (Percie du Sert et al., 2020). Animals had free access to water and either a standard ("normal"; 20% protein, 0.9% lysine) or high lysine (20% protein, 4.7% lysine) diet. At postnatal day 28 (P28), all animals underwent subdural electrode and intrastriatal cannulae implantation (38 males and 28 females). All animals received a normal diet

up to P29. At P30, they were divided into groups according to the diet received: *Gcdh*$^{+/+}$-Lys *(Gcdh*$^{+/+}$ mice receiving high-lysine diet, *n* = 14 males and 12 females); *Gcdh*$^{-/-}$-Lys (*Gcdh*$^{-/-}$ mice receiving high-lysine diet; *n* = 12 males and 10 females); and *Gcdh*$^{-/-}$-*N* (*Gcdh*$^{-/-}$ mice receiving normal diet; *n* = 12 males and 6 females). At P32, they were further divided into six groups according to intrastriatal injection: *Gcdh*$^{+/+}$-Lys-V (*Gcdh*$^{+/+}$-Lys mice receiving vehicle; *n* = 8 males and 4 females); *Gcdh*$^{+/+}$-Lys-QA (*Gcdh*$^{+/+}$-Lys mice receiving QA; *n* = 6 males and 8 females); *Gcdh*$^{-/-}$-Lys-V (*Gcdh*$^{-/-}$-Lys mice receiving vehicle; *n* = 7 males and 2 females); *Gcdh*$^{-/-}$-Lys-QA (*Gcdh*$^{-/-}$-Lys mice receiving QA; *n* = 5 males and 8 females); *Gcdh*$^{-/-}$-N-V (*Gcdh*$^{-/-}$-N mice receiving vehicle; *n* = 5 males and 4 females); and *Gcdh*$^{-/-}$-N-QA (*Gcdh*$^{-/-}$-N mice receiving QA; *n* = 7 males and 2 females).

Randomization of both diet and intrastriatal injection was achieved by assigning a numeric code for each mouse. These codes were then randomly allocated at P30 for each diet (normal or high lysine) and, at P32, for each treatment (vehicle or QA). A slight degree of planning was needed only to assure that at least one mouse in each litter used was assigned to each group. The same numeric codes enabled blinded analyses, as the experimenter was unfamiliar with which codes were allocated for each group.

No relevant differences to our analyses regarding sex were found, therefore male and female mice were assembled together inside every group (Table S1).

2.2 | Electrodes and cannulae implantation

Mice at postnatal day 28 (P28) were anesthetized with ketamine:xylazine (80–120 mg/kg: 10–16 mg/kg, i.p.) for electrode and cannulae implantation (38 males and 28 females). Two recording stainless steel subdural electrodes were bilaterally implanted in the parietal cortex (−2.0 mm AP from the bregma and ±1.2 mm LL) (Paxinos & Franklin, 2001). The reference electrode and one screw for fixation were placed in the occipital bone. Two intrastriatal cannulae were implanted bilaterally (0 mm AP from the bregma, 2.5 mm DV, ±2.5 mm LL) (Paxinos & Franklin, 2001) for posterior injection of either quinolinic acid (QA) or vehicle (V). Dental cement was used to secure the electrodes and cannulae in place. After surgery, each animal was placed individually in an acrylic glass cage for recovery.

2.3 | Video-EEG recordings

At P30, each animal taking the normal diet had its home cage transferred to an observation box, where the electrodes were connected to an amplifier (MAP-32, Plexon, Inc.) and the baseline video-EEG recording was performed for a 20-min period. Afterward, the animals were divided according to the diet intake as explained in detail above. At P32, each animal received, through the intrastriatal cannulae, 1 μl injection of either vehicle (saline, NaCl 0.9%) or 50 mM QA solution (50 nmol; 4.55 nmol/g) dissolved in saline. A 10-μl Gastight® syringe (Hamilton Company) was used to measure the volumes injected and to slowly diffuse the solutions through the cannulae into the striatum of both hemispheres. After the administration, the syringe was left in place for an additional 30-s period and then slowly withdrawn. The dose of QA used was based on previous studies (Amaral et al., 2018; Seminotti et al., 2016). According to the treatment and the diet received, the animals were divided into six final groups as follows: *Gcdh*$^{+/+}$-Lys-V group, *Gcdh*$^{+/+}$-Lys-QA group, *Gcdh*$^{-/-}$-Lys-V group, *Gcdh*$^{-/-}$-Lys-QA group, *Gcdh*$^{-/-}$-N-V group; and *Gcdh*$^{-/-}$-N-QA group. As the high-lysine diet does not induce changes in electrophysiological parameters for *Gcdh*$^{+/+}$ mice (Vendramin Pasquetti et al., 2017), no *Gcdh*$^{+/+}$-N groups were considered for comparison.

Immediately after the injection, a 1-hr period of video-EEG recording was performed for each animal, to evaluate the susceptibility to QA-induced seizures. Latency, duration, and severity of seizures were evaluated by revising the videos and analyzing the EEG recordings. Seizure severity was scored according to the Racine scale (Racine, 1972) and further grouped according to behavioral and electroencephalographic features as stage II-III seizures or stage IV-V seizures. Ictal EEG activity with predominant frequency slower than 10 Hz and amplitude of 1.5 mV or smaller that may or may not be associated with behavioral manifestations was classified as an absence-like seizure (see Figure 1g for representative traces from all severity categories considered). At P34, a 1-hr period of video-EEG was further recorded to confirm whether *Gcdh*$^{-/-}$-Lys mice were able to present SRS as described before (Vendramin Pasquetti et al., 2017) and to evaluate the possible long-term effects of QA injection on brain oscillations.

Sample sizes vary between experiments because of exclusion due to quality of EEG recordings and loss of animals during experiments (i.e., death due to QA injection). The final sample size (at P34) is as follows: *Gcdh*$^{+/+}$-Lys-V, *n* = 8 males and 4 females; *Gcdh*$^{+/+}$-Lys-QA, *n* = 4 males and 7 females; *Gcdh*$^{-/-}$-N-V, *n* = 5 males and 4 females; *Gcdh*$^{-/-}$-N-QA, *n* = 6 males and 2 females; *Gcdh*$^{-/-}$-Lys-V, *n* = 6 males and 2 females; and *Gcdh*$^{-/-}$-Lys-QA, *n* = 4 males and 4 females. Accurate sample sizes for each experiment are specified at Tables S2 and S3.

2.4 | EEG analysis

The qualitative EEG analysis was carried out using the pClamp 10.3 software (Molecular Devices) to identify the QA-induced seizures right after injection in all animals tested and the occurrence of SRS in *Gcdh*$^{-/-}$-Lys mice. The detailed quantitative analysis of power frequencies of EEG recordings was carried out using built-in routines in MATLAB software (Mathworks Inc.). EEG signals were filtered at 0.1–500 Hz followed by digitalization at 1 kHz for posterior analysis. Power spectral density (PSD) analysis was carried out using the *pwelch* function using 4-s Hamming window with 50% overlap (Signal Processing Toolbox). The time–frequency decomposition of all EEG recordings was performed using the *spectrogram* function that uses a Fourier transform. The decomposed signal was quantified in five

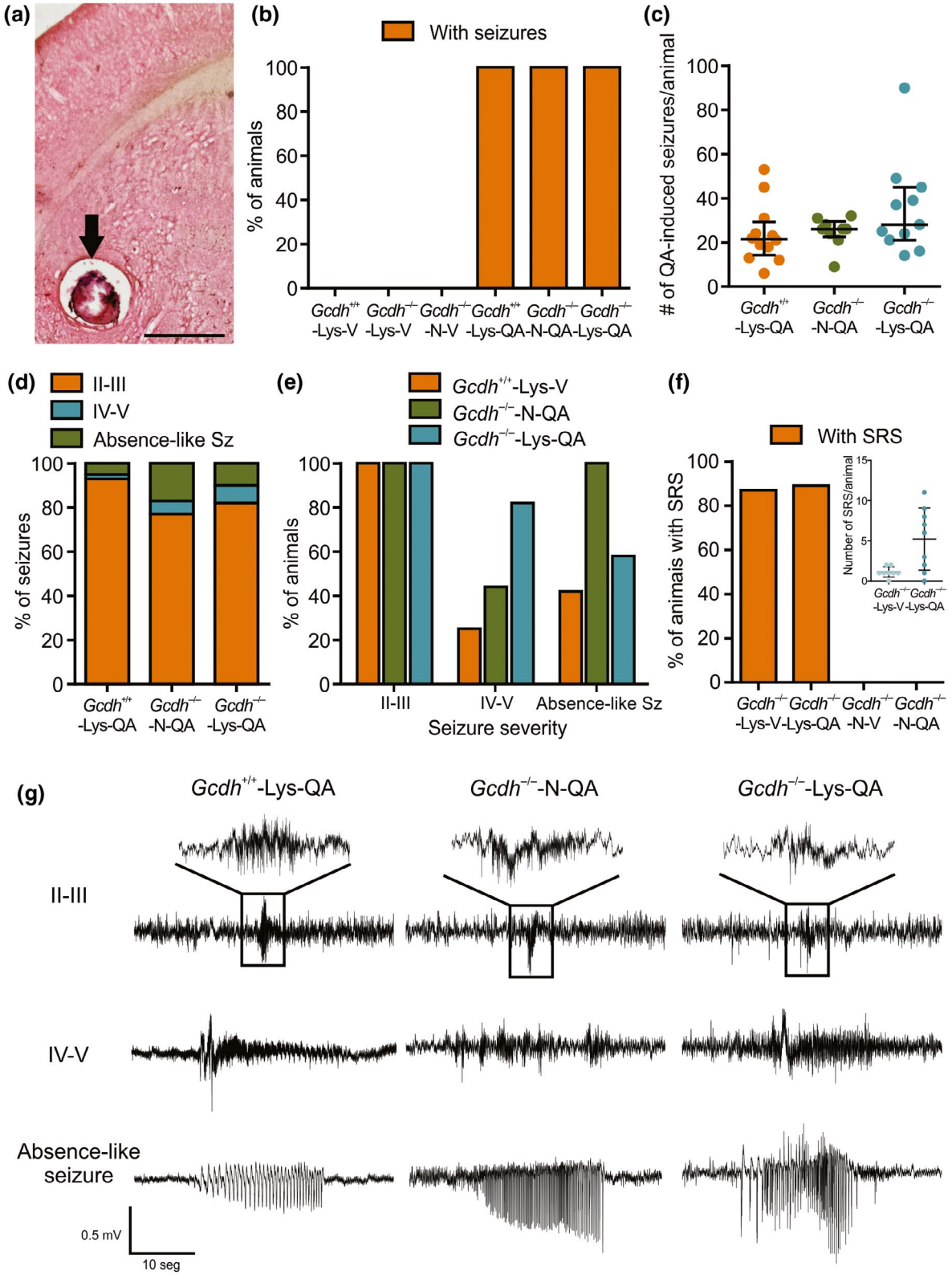

frequency bands: delta (1–4 Hz), theta (4–12 Hz), slow gamma (30–50 Hz), middle gamma (50–90 Hz), and fast gamma (90–150 Hz).

The analysis was performed in two 20-s epochs from baseline recordings (P30) and four 30-s epochs from recordings obtained immediately after the injection (P32) and 4 days after the baseline recordings (P34). Those epochs were chosen, according to the video observation, from moments where the mice were not moving, in order to prevent muscular artifacts on the EEG recordings. The four epochs from EEG recordings taking place immediately after the injection were also chosen after dividing the EEG recordings into four 15-min periods. This strategy was chosen in order to detect the progression of EEG alterations induced by QA injection

FIGURE 1 Increased susceptibility to quinolinic acid (QA)-induced seizures in *Gcdh*$^{-/-}$-Lys mice. (a) Coronal brain slice evidencing the site of cannula implantation (arrow) in the striatum. Scale bar = 500 μm. (b) Percentage of animals with seizures (Sz) following injection of either vehicle (V) or QA. All *Gcdh*$^{+/+}$-Lys-QA ($n = 12$), *Gcdh*$^{-/-}$-Lys-QA ($n = 13$), and *Gcdh*$^{-/-}$-N-QA ($n = 9$) mice had QA-induced Sz, whereas *Gcdh*$^{+/+}$-Lys-V ($n = 12$), *Gcdh*$^{-/-}$-Lys-V ($n = 9$), or *Gcdh*$^{-/-}$-N-V ($n = 9$) mice had no induced Sz ($p < 0.001$). (c) Scatterplots of the number of QA-induced Sz/animal/group during 1-hr electroencephalogram (EEG) recordings after intrastriatal QA injection. The number of Sz was similar for all groups (*Gcdh*$^{-/-}$-Lys-QA: 28 ± 24; *Gcdh*$^{+/+}$-Lys-QA: 21 ± 15; *Gcdh*$^{-/-}$-N-QA: 26 ± 7; $p = 0.21$). (d) Bar plots of percentage of II-III, IV-V, and absence-like Sz for each QA-injected group. *Gcdh*$^{+/+}$-Lys-QA animals developed more II-III stage Sz (93%: 267/287) than other groups (*Gcdh*$^{-/-}$-N-QA: 77%: 170/222; *Gcdh*$^{-/-}$-Lys-QA: 82%: 318/388). *Gcdh*$^{-/-}$-N-QA animals developed more absence-like Sz (17%: 37/222) than other groups (*Gcdh*$^{+/+}$-Lys-QA: 5%: 14/287; *Gcdh*$^{-/-}$-Lys-QA: 10%: 40/388). *Gcdh*$^{-/-}$-Lys-QA animals developed more IV–V stage Sz (8%: 30/388) than other groups (*Gcdh*$^{+/+}$-Lys-QA: 2%: 6/287; *Gcdh*$^{-/-}$-N-QA: 6%: 15/222) ($p = 0.02$). (e) Bar plots of the percentage of animals from each group with II–III, IV–V, and absence-like Sz. A higher percentage of *Gcdh*$^{-/-}$-Lys-QA mice presented IV–V Sz (*Gcdh*$^{-/-}$-Lys-QA: 9/11 animals, 82%; *Gcdh*$^{+/+}$-Lys-QA: 3/12 animals, 25%; *Gcdh*$^{-/-}$-N-QA: 4/9 animals, 44%; $p < 0.001$). All animals from *Gcdh*$^{-/-}$-N-QA mice developed absence-like Sz, while not all mice from the other groups had absence-like Sz (*Gcdh*$^{-/-}$-Lys-QA: 7/11 animals, 58%; *Gcdh*$^{+/+}$-Lys-QA: 5/12 animals, 42%; $p < 0.001$). (f) Percentage of *Gcdh*$^{-/-}$-Lys mice with spontaneous recurrent seizures (SRS) at P34. There was no difference in the number of animals from each group presenting SRS (*Gcdh*$^{-/-}$-Lys-QA: 8/9 mice, 89%; *Gcdh*$^{-/-}$-Lys-V: 7/8 mice, 87%; $p = 0.92$). Inset: Scatterplots of number of SRS at P34/group. *Gcdh*$^{-/-}$-Lys-QA mice developed more SRS than *Gcdh*$^{-/-}$-N-QA mice (*Gcdh*$^{-/-}$-Lys-QA: 5 ± 4 Sz/animal; *Gcdh*$^{-/-}$-Lys-V: 1 ± 1 Sz/animal; $p = 0.01$). (g) Representative EEG traces of QA-induced Sz (II–III, IV–V, and absence-like) at P32. Data are shown as median ± interquartile range

during P32 at 0, 15, 30, and 45 min after the injection, identified in the text by P32/0, P32/15, P32/30, and P32/45, respectively. All epochs were chosen at least 3 min away from electroencephalographic and behavioral seizures. Normalization of quantification values was carried out by dividing the mean power of each frequency band from P32 or P34 epochs by the mean power of all frequency bands in baseline (P30) epochs, which yields a power ratio. Quantitative analyses were also averaged between the two electrodes implanted in each animal.

The EEG left index was calculated as the logarithm of the ratio between the power of the lower frequencies (1–7.4 Hz) and the higher frequencies (13.5–26.5 Hz). Based on values stated by Vogels et al. (1997), normal rats have a left index of approximately 0.6, while left index values of 0.8 or above were considered abnormal. Higher left index values indicate a left shift of the EEG, meaning the predominance of lower frequencies (Bosman et al., 1990), and are indicative of encephalopathy or coma.

The EEG theta/delta ratio was calculated as the power density ratio between theta and delta oscillations in the epochs considered for EEG quantitative analysis. This ratio can be used as an index of cerebral activity (Masuki & Nose, 2009), with lower theta/delta ratio values indicating predominance of delta oscillation power and decreased cerebral activity.

2.5 | Cannulae identification

At the end of the experiments, each animal was euthanized by cervical dislocation and, using a 10-μl Gastight® syringe (Hamilton Company), 1 μl of methylene blue dye was slowly diffused through the cannulae. The brains were removed, left overnight in 4% paraformaldehyde solution, and then stored in 30% sucrose solution at low temperature. Coronal brain slices (60 μm thick) were cut in a cryostat (CM1850, Leica), stained with hematoxylin-eosin and mounted in slides. The position of the cannulae implanted was confirmed by light microscopy, according to methylene blue dye location. Figure 1a shows a brain slice, with methylene blue dye evident in the site of cannulae implantation for intrastriatal QA injection.

2.6 | Statistical analysis

In order to be able to estimate a difference between six groups of animals through the *in vivo* electrophysiological analysis, considering a standard deviation of 25%, with an α of 0.05 and estimated statistical power of 0.8, we calculated that a minimum of six animals *per* group with a real statistical power of 81%. Considering the 10% loss due to anesthesia and 10% loss of electrodes/cannulae implantation, the minimum sample size needed was eight animals *per* group. Sample size calculation was performed using Minitab 17® software.

The normality of data was evaluated using the Shapiro–Wilk test, and statistical tests and data presentation manner were then chosen accordingly. Outliers were defined as data above or below two times the standard deviation calculated, being then removed from further analysis if reaching this threshold.

The effect of QA on seizure induction, seizure severity, SRS, and mortality rate were expressed as percentage and analyzed using Chi-square test. The number of QA-induced seizures, seizure latency, severity, and duration according to severity were expressed as median ± interquartile range and analyzed using Kruskal–Wallis test. The number of SRS was expressed as mean ± *SD* and analyzed using one-way ANOVA and unpaired *t* test. Survival curves for latency for the first QA-induced seizure and mortality rate were analyzed using the log-rank (Mantel–Cox) test. Data from EEG PSD analysis and theta/delta ratio were expressed as median ± interquartile range and analyzed using Scheirer–Ray–Hare extension of the Kruskal–Wallis test followed by Bonferroni's post hoc test and Friedman's two-way analysis of variance. Data from the left index was expressed as mean ± *SD* and analyzed using two-way ANOVA followed by Bonferroni's post hoc test and Friedman's two-way analysis of variance. Statistically significant differences were considered if $p < 0.05$.

FIGURE 2 Differences in seizure latency and duration and mortality profile between groups following quinolinic acid intrastriatal injection. (a) Latency for the first quinolinic acid (QA)-induced seizure. No differences in latency for the first induced seizure were found between groups (*Gcdh*$^{-/-}$-Lys-QA: 4 ± 4.5 min; *Gcdh*$^{+/+}$-Lys-QA: 3 ± 2 min; *Gcdh*$^{-/-}$-N-QA: 4 ± 4 min; $p = 0.67$). (b–e) Scatterplots of duration of seizures in general (b), of stage II–III seizures (c), of stage IV–V seizures (d), and of absence-like seizures (e) for all groups receiving QA. *Gcdh*$^{-/-}$-N-QA mice presented longer seizure duration than other groups (*Gcdh*$^{-/-}$-N-QA: 4.5 ± 7.8 s; *Gcdh*$^{-/-}$-Lys-QA: 2.7 ± 4.0 s; *Gcdh*$^{+/+}$-Lys-QA: 3.7 ± 4.0 s; $p < 0.001$). *Gcdh*$^{-/-}$-Lys-QA mice had shorter II–III seizures than other groups, but this difference is not relevant (*Gcdh*$^{-/-}$-Lys-QA: 2.4 ± 1.9 s; *Gcdh*$^{+/+}$-Lys-QA: 3.4 ± 3.5 s; *Gcdh*$^{-/-}$-N-QA: 3.5 ± 4.7 s; $p < 0.001$). IV-V stages (*Gcdh*$^{-/-}$-Lys-QA: 23.5 ± 26.7 s; *Gcdh*$^{+/+}$-Lys-QA: 22.2 ± 17.7 s; *Gcdh*$^{-/-}$-N-QA: 30.2 ± 20.7 s; $p = 0.22$) and absence-like seizures (*Gcdh*$^{-/-}$-Lys-QA: 16.5 ± 16.9 s; *Gcdh*$^{+/+}$-Lys-QA: 14.2 ± 23.5 s; *Gcdh*$^{-/-}$-N-QA: 11.4 ± 11.3 s; $p = 0.22$) showed no difference in duration between groups. (f) Percentage of animals that died *per* group at P34. The mortality rate of *Gcdh*$^{-/-}$-Lys-QA mice was higher than other groups (*Gcdh*$^{-/-}$-Lys-QA: 4/12 deaths, 33%; *Gcdh*$^{+/+}$-Lys-V: 0/11 deaths, 0%; *Gcdh*$^{+/+}$-Lys-QA: 2/12 deaths, 10%; *Gcdh*$^{-/-}$-N-V: 0/9 deaths, 0%; *Gcdh*$^{-/-}$-N-QA: 1/9 deaths, 11%; *Gcdh*$^{-/-}$-Lys-V: 1/9 deaths, 11%; $p < 0.001$). (g) Survival curve of mortality rate *per* group according to the number of days of diet intake (normal or high lysine). Note that mortality rate increased on the day of QA injection (black arrow). Data are shown as median ± interquartile range. Sz, seizure. $^{*}p < 0.005$; $^{**}p < 0.001$

3 | RESULTS

3.1 | *Gcdh*$^{-/-}$-Lys mice exhibited increased susceptibility to QA-induced seizures and mortality rate

We observed that QA was able to induce seizures in all QA-injected mice, while V-injected mice had no induced seizures (Figure 1b). Two mice from each *Gcdh*$^{+/+}$-Lys-QA and *Gcdh*$^{-/-}$-Lys-QA group presented *status epilepticus* (*SE*), defined as continuous stage IV–V seizures of 5 min or more without returning to less severe stages (Trinka et al., 2015), probably caused by QA injection itself.

We also compared the number, severity, duration, and latency of QA-induced seizures between QA groups. The number of seizures *per* animal was similar (Figure 1c). However, *Gcdh*$^{+/+}$-Lys-QA animals developed more II–III stage seizures, *Gcdh*$^{-/-}$-N-QA animals developed more absence-like seizures, and *Gcdh*$^{-/-}$-Lys-QA animals developed more IV–V stage seizures than other groups (Figure 1d).

While animals of all groups developed II–III stage seizures, the percentage of *Gcdh*$^{-/-}$-Lys-QA animals with IV–V stage seizures was higher than in the other groups (Figure 1e). All *Gcdh*$^{-/-}$-N-QA animals, but not all *Gcdh*$^{-/-}$-Lys-QA and *Gcdh*$^{+/+}$-Lys-QA animals, developed absence-like seizures (Figure 1e). Figure 1g shows representative EEG traces for all seizure types according to severity stage for each group.

At P34, *Gcdh*$^{-/-}$-Lys, but not *Gcdh*$^{-/-}$-N mice, developed SRS (Figure 1f). While no difference was found in the number of mice with SRS (Figure 1f), the number of SRS *per* animal was higher in *Gcdh*$^{-/-}$-Lys-QA group (Figure 1f inset).

No differences in latency for the first QA-induced seizure were found between groups (Figure 2a).

Gcdh$^{-/-}$-N-QA mice had longer seizures than the other groups (Figure 2b). *Gcdh*$^{-/-}$-Lys-QA animals had shorter duration of II–II stage seizures than the other groups (Figure 2c). However, this difference of only about 1 s is not relevant and is hereby not considered. No differences between groups were observed for duration of IV-V stages or absence-like seizures (Figure 2d,e, respectively).

Finally, the mortality rate of *Gcdh*$^{-/-}$-Lys-QA mice was higher than all other groups (Figure 2f). Two *Gcdh*$^{+/+}$-Lys-QA and one *Gcdh*$^{-/-}$-N-QA mice died right after QA injection, most likely due to QA injection itself (Figure 2g, black arrow).

Taken together, our data indicate that *Gcdh*$^{-/-}$-Lys mice had increased susceptibility to QA, as they presented more seizures of higher severity stages following injection and, at long term, increased number of SRS at P34.

3.2 | QA-induced changes in brain oscillations

No differences were found for power of delta between groups (P32/0: $F_{2,47} = 0.71$, $p = 0.50$; P32/15: $F_{2,47} = 0.795$, $p = 0.46$; P32/30: $F_{2,47} = 0.104$, $p = 0.90$; P32/45: $F_{2,47} = 0.192$, $p = 0.83$; P34: $F_{2,40} = 1.93$, $p = 0.16$; Figure 3a–e, Table S2). Conversely, QA groups displayed lower theta power than V groups at P32/0 ($F_{1,47} = 32.13$, $p < 0.05$), P32/15 ($F_{1,47} = 37.67$, $p < 0.05$), and P32/30 ($F_{1,47} = 31.79$, $p < 0.05$; Figure 3a–e, Table S2), while no differences were found at P32/45 ($F_{2,47} = 0.413$, $p = 0.66$) and P34 ($F_{2,40} = 0.503$, $p = 0.61$).

Similar to theta, QA groups presented lower power of slow gamma at P32/0 ($F_{1,47} = 25.35$, $p < 0.05$), P32/15 ($F_{1,47} = 43.12$, $p < 0.05$), and P32/30 ($F_{1,47} = 33.17$, $p < 0.05$; Figure 4a–e, Table S2) than V groups. No differences were found at P32/45 ($F_{2,47} = 0.60$, $p = 0.55$) or P34 ($F_{2,40} = 0.33$, $p = 0.72$). No differences were found in the power of middle gamma (P32/0: $F_{2,47} = 0.46$, $p = 0.63$; P32/15: $F_{2,47} = 0.04$, $p = 0.96$; P32/30: $F_{2,47} = 0.68$, $p = 0.51$; P32/45: $F_{2,47} = 0.80$, $p = 0.46$; P34: $F_{2,40} = 1.135$, $p = 0.33$; Figure 4, Table S2) and fast gamma (P32/0: $F_{2,47} = 0.64$, $p = 0.53$; P32/15: $F_{2,47} = 0.17$, $p = 0.84$; P32/30: $F_{2,47} = 1.52$, $p = 0.23$; P32/45: $F_{2,47} = 1.91$, $p = 0.16$; P34: $F_{2,40} = 1.125$, $p = 0.34$; Figure 4, Table S2).

Over time, all QA-injected groups and *Gcdh*$^{-/-}$-N-V had increased power of delta oscillation at P34 when compared to P32/0. Delta power also increased at P34 in *Gcdh*$^{-/-}$-Lys-QA and *Gcdh*$^{+/+}$-Lys-QA groups when compared to P32/15. No differences were found for *Gcdh*$^{-/-}$-Lys-V and *Gcdh*$^{+/+}$-Lys-V animals (Figure S1a).

The power of theta oscillation increased in all groups, except *Gcdh*$^{-/-}$-Lys-V, at P34 over P32/0, and in all QA groups over P32/15. In *Gcdh*$^{+/+}$-Lys-QA, *Gcdh*$^{-/-}$-N-QA, *Gcdh*$^{+/+}$-Lys-V, and *Gcdh*$^{-/-}$-N-V animals, theta power increased at P32/45 when compared to P32/0.

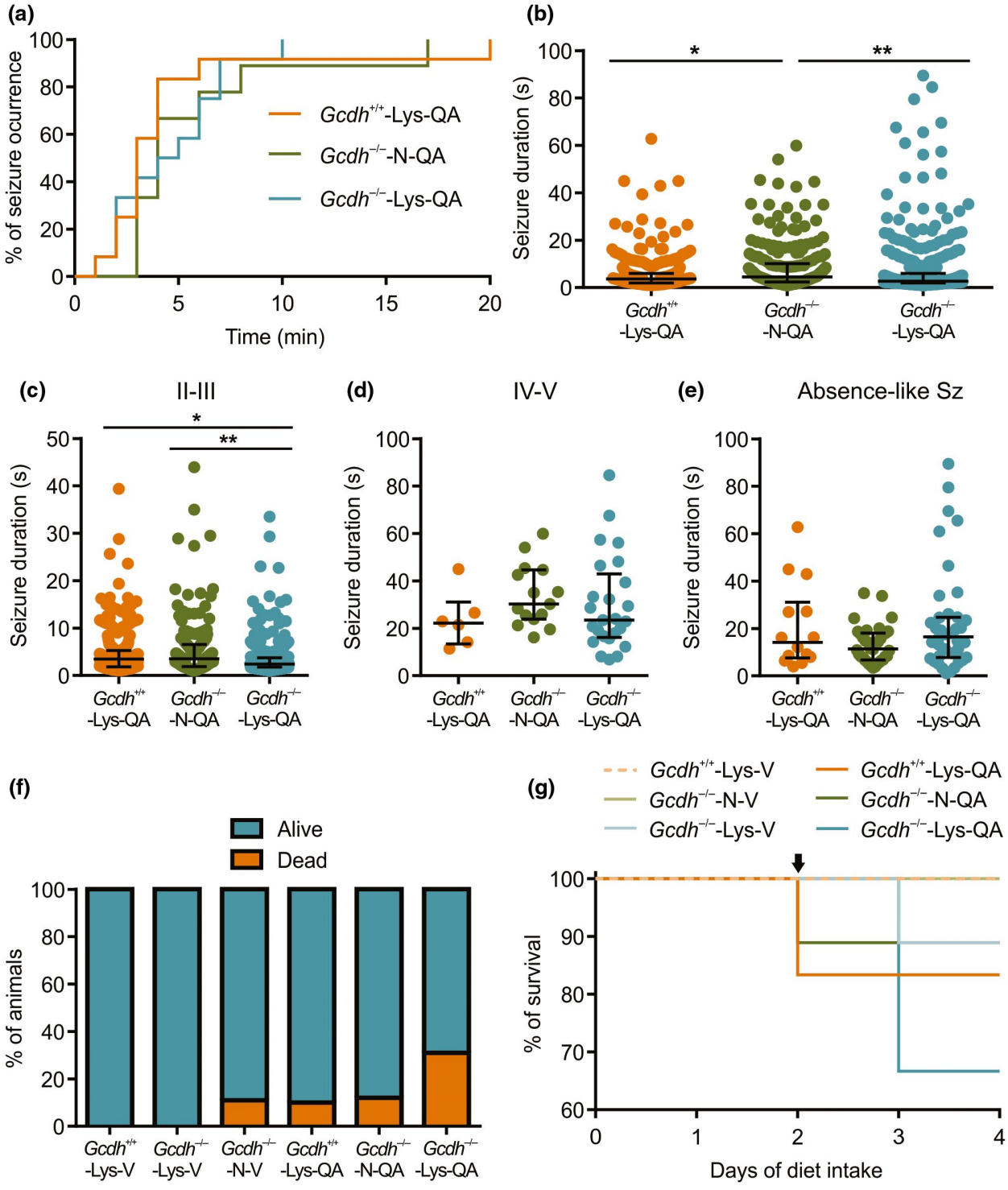

Theta power in *Gcdh*$^{+/+}$-Lys-QA mice also increased at P32/30 over P32/0 and at P34 over P32/30, while in *Gcdh*$^{-/-}$-Lys-QA animals, it increased at P32/45 over P32/15. No differences were found for *Gcdh*$^{-/-}$-Lys-V animals (Figure S1b).

The power of slow gamma oscillation increased in all groups at P34 when compared to P32/0 and in all groups, except *Gcdh*$^{-/-}$-Lys-V, when compared to P32/15. Slow gamma power also increased in *Gcdh*$^{+/+}$-Lys-QA, *Gcdh*$^{-/-}$-N-QA, and *Gcdh*$^{+/+}$-Lys-V animals at P32/45 when compared to P32/0 and in *Gcdh*$^{-/-}$-Lys-QA and *Gcdh*$^{+/+}$-Lys-QA animals when compared to P32/15. Finally, in *Gcdh*$^{+/+}$-Lys-QA, *Gcdh*$^{+/+}$-Lys-V, and *Gcdh*$^{-/-}$-N-V animals, the power of slow gamma increased at P32/30 over P32/0 (Figure S1c).

The power of middle gamma oscillation increased in all groups at P34 over P32/0; for all groups, except *Gcdh*$^{-/-}$-Lys-V, over P32/15; in *Gcdh*$^{-/-}$-Lys-V group over P32/30; and in V-injected groups

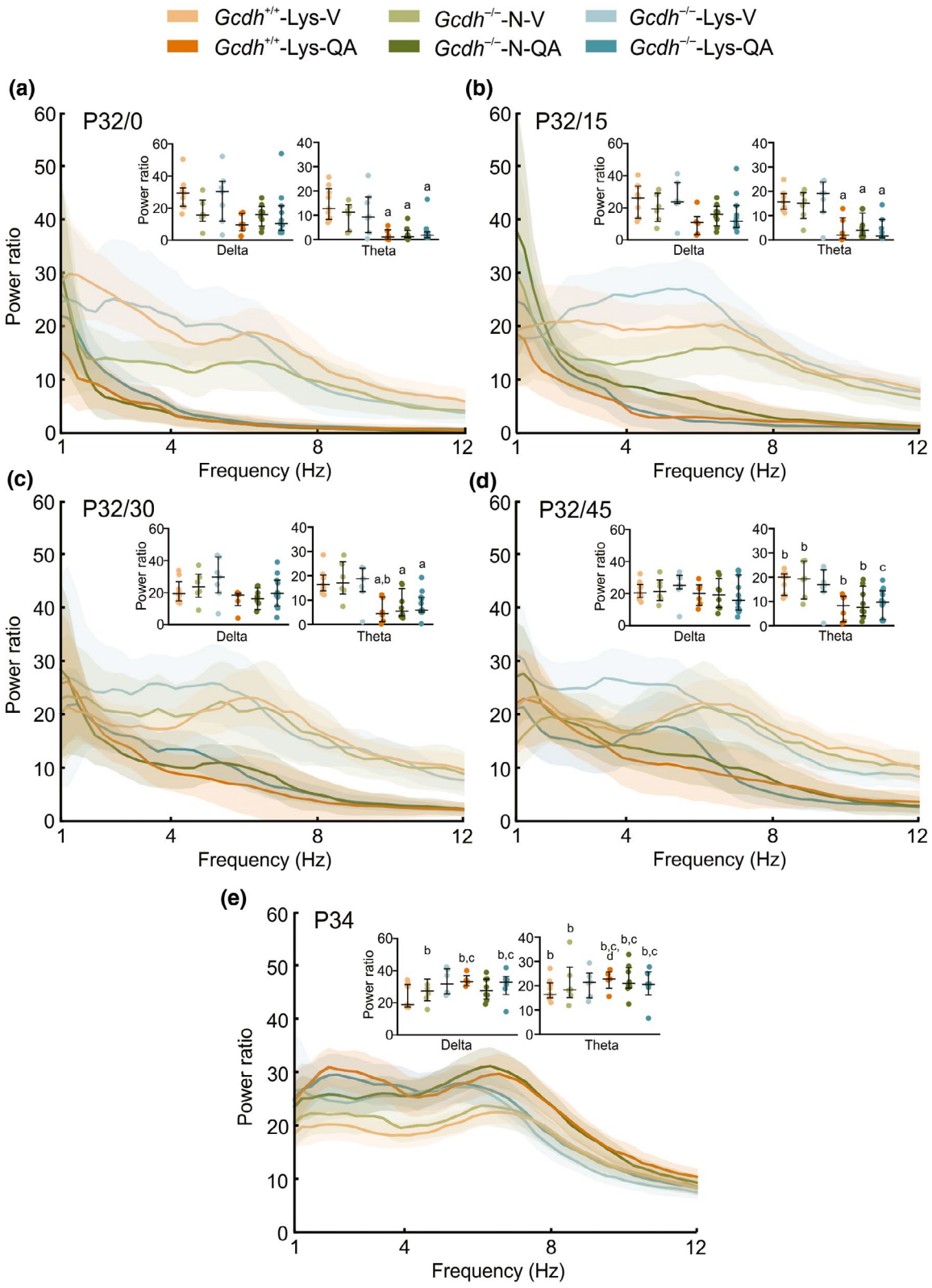

when compared to P32/45. The power of middle gamma increased in *Gcdh*$^{-/-}$-N-QA, *Gcdh*$^{+/+}$-Lys-QA, and *Gcdh*$^{+/+}$-Lys-V animals at P32/45 over P32/0 and in *Gcdh*$^{+/+}$-Lys-QA animals when compared to P32/15. *Gcdh*$^{+/+}$-Lys-QA and *Gcdh*$^{+/+}$-Lys-V animals also showed increased middle gamma power at P32/30 over P32/0 (Figure S1d).

The power of fast gamma increased in all groups at P34 when compared to P32/0; in all groups, except *Gcdh*$^{-/-}$-Lys-V, over P32/15; in *Gcdh*$^{-/-}$-Lys-V mice when compared to P32/45; and in *Gcdh*$^{+/+}$-Lys-V mice when compared to P32/30 and P32/45. *Gcdh*$^{-/-}$-N-QA mice also showed increased fast gamma power at P32/45 over P32/0 (Figure S1e).

FIGURE 3 Changes in the power of delta and theta oscillations after quinolinic acid intrastriatal injection. Power ratio plots of delta and theta oscillations between groups treated with vehicle (V) or quinolinic acid (QA) at P32/0 (a), P32/15 (b), P32/30 (c), P32/45 (d), and P34 (e). No differences were found for the power of delta between groups at all time points ($p = 0.50$, $p = 0.46$, $p = 0.90$, $p = 0.83$, $p = 0.16$, respectively). Note the lower power values for theta oscillations of animals receiving QA at P32/0, P32/15, and P32/30 ($p < 0.05$ for all) with no difference at P32/45 and P34 ($p = 0.66$ and $p = 0.61$, respectively). Scatterplots also show differences between distinct time periods for the same group. Data are shown as median ± interquartile range. Scheirer–Ray–Hare extension of the Kruskal–Wallis test followed by Bonferroni's post hoc test was used for statistical comparison between genotype + diet and treatments: [a]$p < 0.05$ from saline, among the same genotype + diet. [b–e]Friedman's two-way analysis of variance was used for statistical comparison between different time periods for the same group: [b]$p < 0.05$ from P32/0; [c]$p < 0.05$ from P32/15; [d]$p < 0.05$ from P32/30; [e]$p < 0.05$ from P32/45 min

3.3 | *Gcdh*$^{-/-}$-Lys-QA mice show predominance of slow brain oscillations

In order to expand EEG quantitative analyses, the left index and theta/delta ratio were also determined (Figure 5, Table S3). At baseline, no differences between groups were found ($F_{2,50} = 0.162$, $p = 0.85$). However, at all P32 time periods, QA groups had higher left index than their respective V groups (P32/0: $F_{1,50} = 13.12$, $p = 0.001$; P32/15: $F_{1,50} = 46.47$, $p < 0.001$; P32/30: $F_{1,50} = 25.32$, $p < 0.001$; P32/45: $F_{1,50} = 31.745$, $p < 0.001$). At P32/15, *Gcdh*$^{-/-}$-Lys mice also presented higher left index than *Gcdh*$^{+/+}$-Lys mice ($F_{2,50} = 10.31$, $p < 0.001$). At P32/30 and P32/45, *Gcdh*$^{-/-}$-Lys and *Gcdh*$^{-/-}$-N mice also had higher left index than *Gcdh*$^{+/+}$-Lys mice (P32/30: $F_{2,50} = 9.53$, $p < 0.001$; P32/45: $F_{2,50} = 18.975$, $p < 0.001$). Finally, at P34, *Gcdh*$^{-/-}$-Lys-V mice had higher left index than both *Gcdh*$^{-/-}$-N-V and *Gcdh*$^{+/+}$-Lys-V; and *Gcdh*$^{-/-}$-Lys-QA and *Gcdh*$^{-/-}$-N-QA mice had higher left index than *Gcdh*$^{+/+}$-Lys-QA ($F_{2,45} = 3.79$, $p = 0.03$; Figure 5a, Table S3).

We also evaluated left index values over time (Figures 5a, S2a and Table S3). *Gcdh*$^{-/-}$-Lys-QA, *Gcdh*$^{-/-}$-Lys-V, and *Gcdh*$^{+/+}$-Lys-QA mice showed increased left index at P32/0 when compared to baseline. Only *Gcdh*$^{-/-}$-Lys-QA animals, however, remained with increased left index values at P32/15. In all QA groups, left index decreased at P34 when compared to P32/0, and in *Gcdh*$^{-/-}$-Lys-QA and *Gcdh*$^{+/+}$-Lys-QA animals, over P32/15. *Gcdh*$^{+/+}$-Lys-V mice had decreased left index over P32/0 at P32/15, P32/30, and P32/45, while *Gcdh*$^{+/+}$-Lys-V mice had decreased left index over P32/0 at P32/45. No differences were found for *Gcdh*$^{-/-}$-N-V mice.

No significant differences were found between groups at baseline for theta/delta ratio ($F_{2,51} = 3.52$, $p > 0.05$). At P32/0 and P32/15, QA groups had lower theta/delta ratio than the respective V groups (P32/0: $F_{1,51} = 23.10$, $p < 0.05$; P32/15: $F_{1,51} = 31.65$, $p < 0.02$), with no differences after this time period (P32/30: $F_{2,51} = 0.06$, $p = 0.94$; P32/45: $F_{2,51} = 0.06$, $p = 0.95$; P34: $F_{2,44} = 0.933$, $p = 0.40$; Figure 5b, Table S3).

No differences in theta/delta ratio were found over time in *Gcdh*$^{-/-}$-Lys-V animals. In all QA groups and *Gcdh*$^{+/+}$-Lys-V animals at P32/0 and in *Gcdh*$^{-/-}$-Lys-QA and *Gcdh*$^{-/-}$-N-QA animals at P32/15, theta/delta ratio decreased when compared to baseline. However, theta/delta ratio started to increase after P32/15. In *Gcdh*$^{+/+}$-Lys groups, the ratio increased at P32/30, P32/45, and P34 when compared to P32/0. In *Gcdh*$^{-/-}$-Lys-QA and in *Gcdh*$^{-/-}$-N-V groups, it increased at P32/45 over P32/15 and P32/0, respectively. Finally, in *Gcdh*$^{-/-}$-Lys-QA, *Gcdh*$^{-/-}$-N-QA, and *Gcdh*$^{-/-}$-Lys-V animals, it increased at P34 when compared to P32/0; and in *Gcdh*$^{-/-}$-Lys-QA group, it increased when compared to P32/15 (Figures 5b, S2b, Table S3).

4 | DISCUSSION

Here we investigated the effects of intrastriatal QA injection on EEG and seizure behavior of an animal model of GA-I, the *Gcdh*$^{-/-}$-Lys mice. Our main findings include increased susceptibility to seizures and mortality rate and changes in cortical oscillations of *Gcdh*$^{-/-}$-Lys mice, such as decreased the power of theta and slow gamma oscillations and long-term increment of left index, which characterize an ongoing encephalopathy.

4.1 | Long-term effects of acute QA administration in *Gcdh*$^{-/-}$-Lys mice

Although the number of QA-induced seizures was similar between groups, *Gcdh*$^{-/-}$-Lys-QA mice developed more seizures of high severity. As the intracerebroventricular injection of QA at the same dosage used in this study was shown to induce tonic-clonic seizures in 50% of wild-type young rats (Oliveira et al., 2004), our result may indicate an increased susceptibility of *Gcdh*$^{-/-}$-Lys mice QA-induced seizures of higher severity.

Although *Gcdh*$^{-/-}$-Lys mice receiving either vehicle or QA developed SRS at P34, as expected based on a previously published study by our group (Vendramin Pasquetti et al., 2017), the number of SRS in QA-treated mice was higher. The mortality rate of *Gcdh*$^{-/-}$-Lys-QA mice at P34 was also higher than in the other groups. These findings may indicate that the excitotoxicity induced by acute administration of QA remains for a longer period in the GA-I animal model, as the high-lysine diet itself was notable to induce such long-term outcomes.

The increased number of absence-like seizures, which lasted longer than the other seizure types evaluated here, can explain the longer seizure duration of *Gcdh*$^{-/-}$-N-QA mice. Recent evidence suggests that loss of inhibition can be involved in absence-like seizure generation (Panthi & Leitch, 2019). Interestingly, QA is known to impair the GABAergic system in multiple ways. QA is known to induce the degeneration of GABAergic interneurons and projections, as well as the loss of $GABA_A$ receptors in neuronal

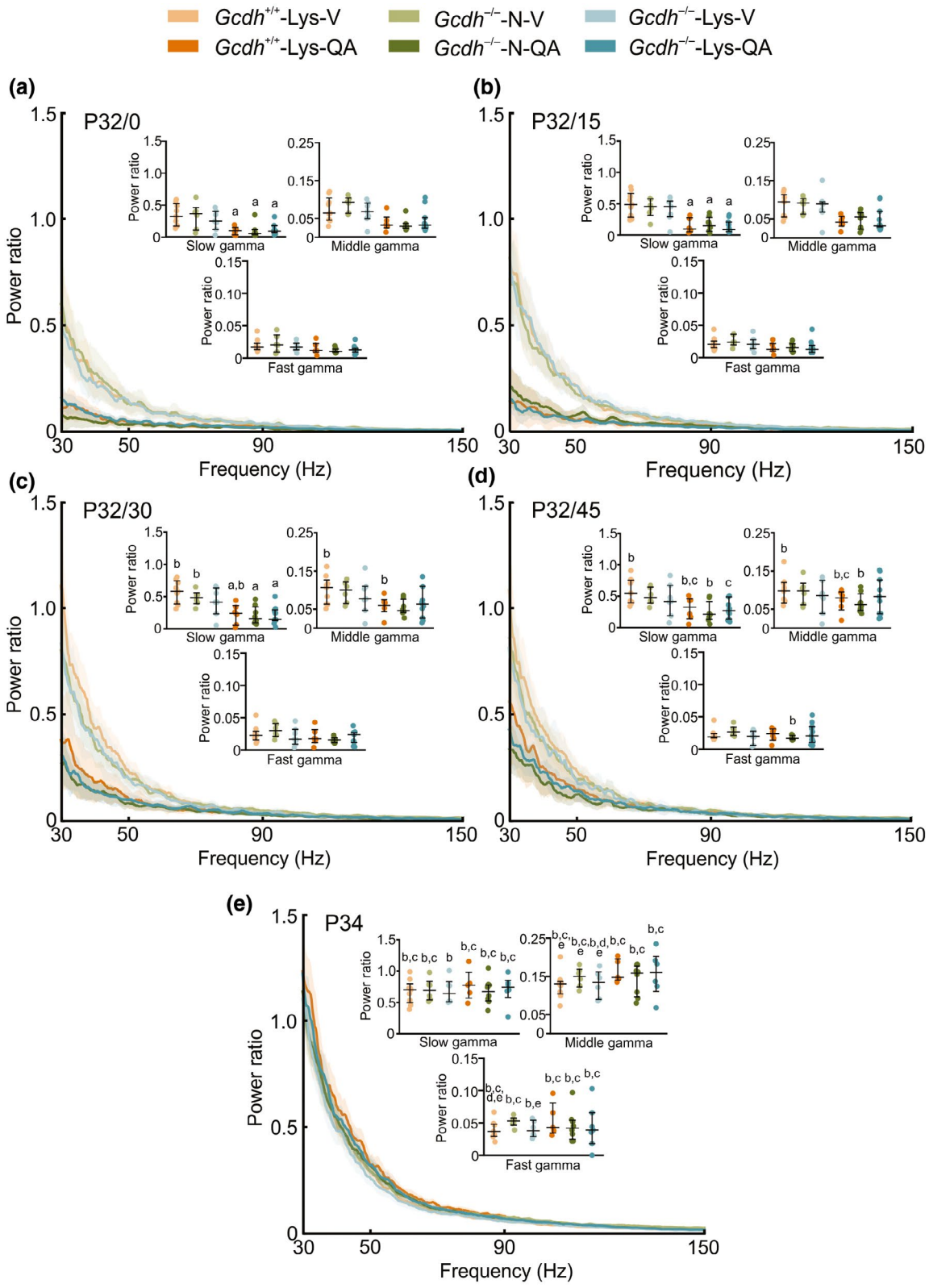

and glial cells and chronic depletion of extracellular GABA levels (Brickell et al., 1999; Pierozan et al., 2014; Reynolds et al., 1997). Also, in a previous study, we were able to demonstrate a decreased GABA release associated with a decrease in GAD immunocontent and activity and reduced inhibitory synaptic transmission in the neocortex of both *Gcdh*$^{-/-}$-Lys and *Gcdh*$^{-/-}$-N mice (Vendramin Pasquetti et al., 2017). It is then possible that *Gcdh*$^{-/-}$ mice, regardless of the diet received, endure a combined effect of QA and intrinsic loss of inhibition, which could contribute to the development of absence-like seizures.

FIGURE 4 Changes in the power of slow, middle, and fast gamma oscillations after quinolinic acid intrastriatal injection. Power ratio plots of slow, middle, and fast gamma oscillations between groups treated with vehicle (V) or quinolinic acid (QA) at P32/0 (a), P32/15 (b), P32/30 (c), P32/45 (d), and P34 (e). Note the lower power values of slow gamma of animals receiving QA at P32/0, P32/15, and P32/30 ($p < 0.05$ for all). No differences were found at P32/45 and P34 ($p = 0.55$ and $p = 0.72$, respectively). Also, no differences were found in the power of middle gamma ($p = 0.63$, $p = 0.96$, $p = 0.51$, $p = 0.46$ and $p = 0.33$) and fast gamma ($p = 0.53$, $p = 0.84$, $p = 0.23$, $p = 0.16$ and $p = 0.34$) between groups at all periods (P32/0, P32/15, P32/30, P32/45 and P34, respectively). Scatterplots also show differences between distinct time periods for the same group. Data are shown as median ± interquartile range. [a]Scheirer–Ray–Hare extension of the Kruskal–Wallis test followed by Bonferroni's post hoc test was used for statistical comparison between genotype + diet and treatments: [a]$p < 0.05$ from saline, among the same genotype + diet. [b–e]Friedman's two-way analysis of variance was used for statistical comparison between different time periods for the same group: [b]$p < 0.05$ from P32/0; [c]$p < 0.05$ from P32/15; [d]$p < 0.05$ from P32/30; [e]$p < 0.05$ from P32/45

4.2 | Changes in power spectral density of cortical oscillations after QA injection

Our results show that QA impaired both theta and slow gamma oscillations after acute treatment in comparison to vehicle-treated mice, while no alterations were seen for delta, middle gamma, and fast gamma rhythms between groups at P32 or at a long-term analysis (P34). As both theta and gamma rhythms in the striatum had been related to cognitive tasks (Tort et al., 2008), the decrease in the power of theta oscillation could be correlated with cognitive impairments seen in the animal model (Koeller et al., 2002) and in patients with GA-I (Wajner, 2019).

Theta and gamma rhythms are markedly regulated by GABAergic interneuron activity (Buzsáki, 2006; Buzsáki & Wang, 2012). Interestingly, the GABAergic system is impaired in the striatum following local acute QA injection (Beal et al., 1986). Previous studies hypothesize that distinct populations of inhibitory interneurons may be responsible for generating distinct gamma rhythms (Lasztóczi & Klausberger, 2014; van der Meer, 2009), and certain types of striatal interneurons seem to be more susceptible to QA excitotoxicity than others (Feng et al., 2014). This may explain why slow gamma, but not middle and fast gamma oscillations, was impaired following QA injection. However, the specific relation between striatal interneuron subtypes and distinct gamma rhythms is still to be explored.

All vehicle and QA-treated groups showed decreased power values for all frequency bands immediately after injection. It is possible to assume that the injection procedure *per se* and the volume injected are responsible for this transient decrease. A similar finding was reported before, where intrahippocampal injection of either saline or QA induced transient decreases in EEG amplitude right after the procedure (Schwarcz et al., 1984). Although intracerebral injection is a reliable way for drug delivery, the vehicles injected can exert transient effects *per se*, including cell damage and displacement (Robinson, 1969; Yaksh et al., 1991). Even though saline is assumed to be isotonic, it alters the extracellular ionic balance of the surrounding region and, consequently, cell volume (Sabel et al., 1985) and brain activity (Hübel & Ullah, 2016; Ullah et al., 2015; Wilson & Mongin, 2018).

4.3 | Increases in EEG left index and decreases in theta/delta ratio values

The EEG left index analysis represents left shifts in the PSD of cortical oscillations, and high left index (>0.8) values are related to neurological damage, encephalopathy, and coma (Bosman et al., 1990; Vogels et al., 1997). QA treatment caused an immediate increase in left index for all groups, but only *Gcdh*$^{-/-}$-Lys-QA and *Gcdh*$^{-/-}$-N-QA groups remained with values above the normal threshold (Vogels et al., 1997) through P32 recording. Also, left index values remained higher for *Gcdh*$^{-/-}$-Lys-QA and *Gcdh*$^{-/-}$-N-QA mice at P34 over other groups. These results may imply an increased sensibility to QA for both *Gcdh*$^{-/-}$ groups, regardless of diet. Thus, QA administration can act similar to lysine overload, simulating acute catabolic states that contribute to severe neurological features seen in patients with GA-I (Wajner, 2019).

All groups showed a decrease in theta/delta ratio after the injection procedure, which was quickly reverted to baseline values for vehicle-treated groups. This can attributed to the injection procedure and volume of solution injected (Ullah et al., 2015), and that was similar to what we had observed for the power values for all frequency bands immediately after injection. Conversely, theta/delta ratio decreased in all QA-injected groups up to 30 min after injection as a consequence of decreased power values of theta oscillation, suggesting an impairment of brain activity (Masuki & Nose, 2009).

Similar to left index values, no differences were found for theta/delta ratio between P34 and baseline. As up to one third (33%) of *Gcdh*$^{-/-}$-Lys-QA mice died before reaching P34 due to QA and high-lysine diet effects, our group of *Gcdh*$^{-/-}$-Lys animals could be clustered in "more susceptible" and "less susceptible" groups to QA and/or diet. Therefore, supposing that mortality rate at P34 was particularly high among the "more susceptible" group, *Gcdh*$^{-/-}$-Lys-QA animals evaluated at P34 could not display severe changes in brain oscillations. This hypothesis is corroborated by previous studies where QA, at the same concentration used here, induced variable susceptibility to seizures in rats (Oliveira et al., 2004). Also, some mice have high tolerance to diet intake and do not develop a GA-I phenotype (Zinnanti et al., 2006). However, the mechanism for such differences in QA or high-lysine diet susceptibility among *Gcdh*$^{-/-}$ mice are still unclear.

In this study, not all *Gcdh*$^{-/-}$ mice develop the full GA-I phenotype after high-lysine diet intake and no way of assessing which animals would be resistant to developing GA-I was possible. Therefore, resistant mice are a limitation of the animal model used and could be a source of bias for our results. In addition, we tried as much as possible not to select specific mice from litters, sometimes leading to discrepancies between the number of male and female mice used,

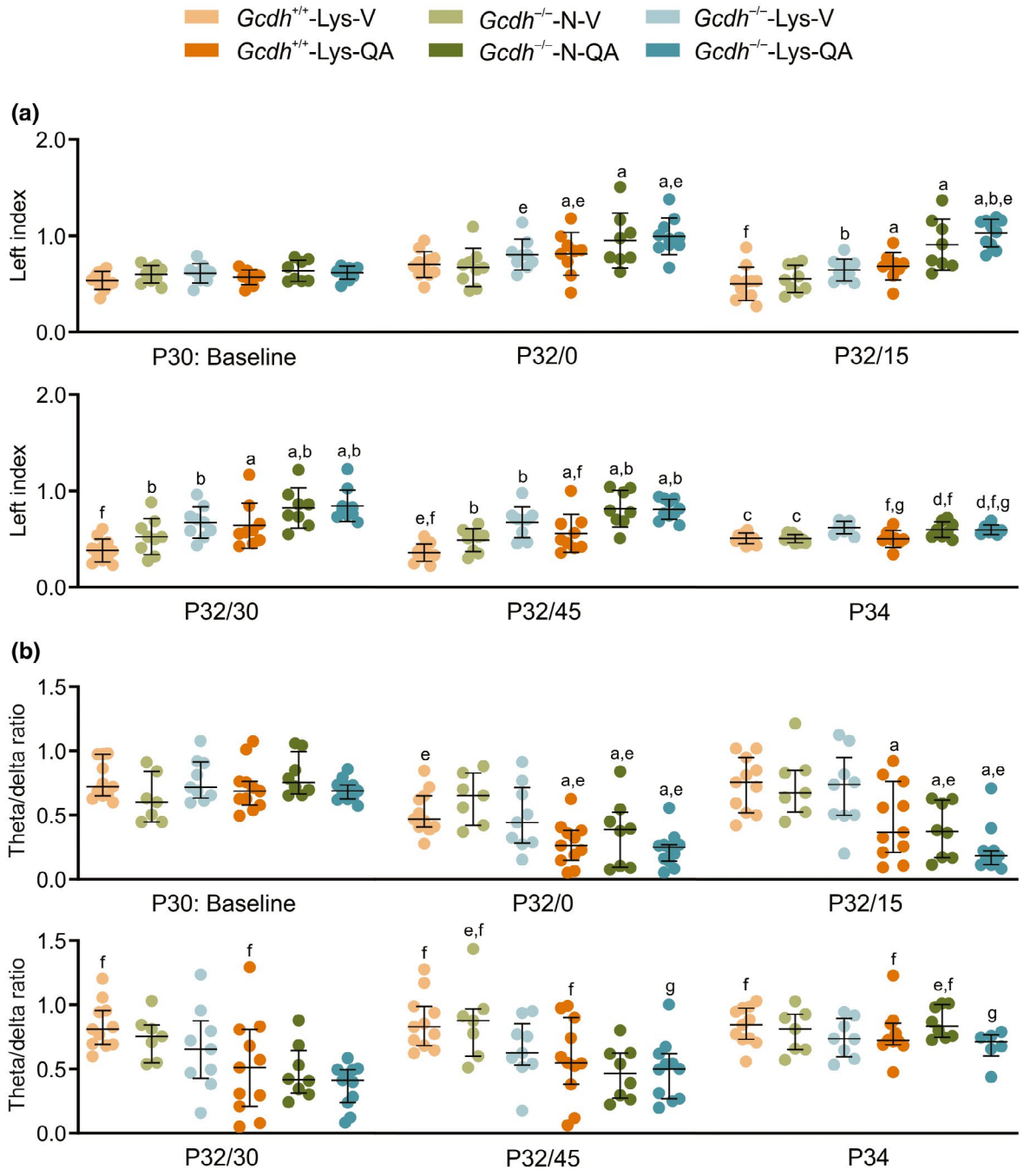

FIGURE 5 Effects of intrastriatal quinolinic acid injection on brain activity indices. Scatterplots showing differences in left index (a) and theta/delta ratio (b) between groups at the same time period or among the same group between different time periods analyzed. (a) Note that, during P32 time periods, quinolinic acid (QA)-groups had higher left index than vehicle (V)-groups (P32/0, $p = 0.001$; P32/15, P32/30 and P32/45, $p < 0.001$). From P32/15 to P32/45, *Gcdh*$^{-/-}$-Lys mice had higher left index than *Gcdh*$^{+/+}$-Lys mice ($p < 0.001$) and, at P32/30 and P32/45, *Gcdh*$^{-/-}$-N mice also had higher left index than *Gcdh*$^{+/+}$-Lys mice ($p < 0.001$). At P34, *Gcdh*$^{-/-}$-Lys-V mice had higher left index than *Gcdh*$^{-/-}$-N-V and *Gcdh*$^{+/+}$-Lys-V groups; and *Gcdh*$^{-/-}$-Lys-QA and *Gcdh*$^{-/-}$-N-QA mice had higher left index than *Gcdh*$^{+/+}$-Lys-QA groups ($p = 0.03$). Left index values at the baseline period were similar in all groups ($p = 0.85$). (b) Note that, at P32/0 and P32/15, QA groups had lower theta/delta ratio than the respective V groups (P32/0: $p < 0.05$; P32/15: $p < 0.02$), with no differences at baseline ($p > 0.05$) and after P32/15 (P32/30: $p = 0.94$; P32/45: $p = 0.95$; P34: $p = 0.40$). Data are shown as mean ± *SD* for left index and median ± interquartile range for theta/delta ratio. [a–d]Two-way ANOVA followed by Bonferroni's post hoc test for left index and Scheirer–Ray–Hare extension of the Kruskal–Wallis test followed by Bonferroni's post hoc test for theta-delta ratio were used for statistical comparison between genotype + diet and treatments: [a]$p < 0.05$ from vehicle, among the same genotype + diet; [b]$p < 0.05$ from *Gcdh*$^{+/+}$-Lys, among the same treatment; [c]$p < 0.05$ from *Gcdh*$^{-/-}$-Lys-V, with interaction between genotype + diet and treatment; [d]$p < 0.05$ from *Gcdh*$^{+/+}$-Lys-QA, with interaction between genotype + diet and treatment. [e–g]Friedman's two-way analysis of variance was used for statistical comparison between different time periods for the same group: [e]$p < 0.05$ from P30; [f]$p < 0.05$ from P32/0; [g]$p < 0.05$ from P32/15

which could potentially hinder the possibility of assessing proper sex differences. Despite the limitations, our key findings including the increased seizure susceptibility, changes in cortical oscillation patterns, and increased mortality rate following high-lysine diet intake and QA injection in GCDH-deficient mice may contribute to the hypothesis of QA involvement in the neurological features in GA-I, particularly in the ictogenesis during acute episodes of encephalopathy, commonly elicited by infection.

The present study demonstrated a higher susceptibility of the genetic mouse model of GA-I to QA, as revealed by the severe seizures observed in these animals relative to the controls when injected intrastriatally with this potent neurotoxin NMDA receptor agonist. If these findings could be translated to the human condition, it would be tempting to speculate that endogenous QA, produced by microglial cells in the central nervous system, as one endpoint of the kynurenine pathway of tryptophan degradation (Maddison & Giorgini, 2015), could act synergically at NMDA receptors, with other organic acids, whose synthesis is increased in GA-I patients, causing excitotoxic neuronal cell damage and striatal necrosis. In fact, this association may ultimately lead to the characteristic seizures induced by episodes of acute encephalopathy during infections/inflammatory processes observed in GA-I patients, as originally proposed (Varadkar & Surtees, 2004). Although there is unclear evidence of QA involvement in GA-I in humans, quantifying kynurenine pathway metabolites in biological fluids of patients with GA-I under different stages of the disease, as well as in postmortem brain structures to detect regional-specific, disease-related alterations of this pathway, would be a valuable method to investigate the pathogenesis and potential peripheral biomarkers of GA-I progression.

DECLARATION OF TRANSPARENCY

The authors, reviewers and editors affirm that in accordance to the policies set by the *Journal of Neuroscience Research*, this manuscript presents an accurate and transparent account of the study being reported and that all critical details describing the methods and results are present.

ACKNOWLEDGMENTS

This work was supported by Conselho Nacional de Desenvolvimento Científico e Tecnológico (CNPq), Brazil [grant number 465671/2014-4] and Coordenação de Aperfeiçoamento de Pessoal de Nível Superior (CAPES). We thank Dr Stephen Goodman, former researcher of University of Colorado Denver, for the conceptualization of the initial work (in memoriam).

CONFLICT OF INTEREST

The authors have no conflict of interest to declare.

AUTHOR CONTRIBUTIONS

All the authors take responsibility for the integrity of the data and the accuracy of the data analysis. *Conceptualization*, M.E.C., L.B.C., and M.Wa.; *Methodology*, L.B.C., M.V.P., B.S., and M.E.C.; *Software*, L.B.C. and M.V.P.; *Investigation*, L.B.C., M.V.P., and M.E.C.; *Formal Analysis*, L.B.C., M.V.P., and M.E.C.; *Writing – Original Draft*, L.B.C. and M.E.C.; *Writing – Review & Editing*, L.B.C., M.V.P., M.Wa., M.Wo., and M.E.C.; *Visualization*, L.B.C. and M.E.C.; *Supervision*, M.E.C.; *Project Administration*, M.E.C.

ETHICAL APPROVAL

All procedures were approved and performed according to the Brazilian legal guidelines (Law #11.794/2008) and the Ethics Committee for the Care and Use of Laboratory Animals of Hospital de Clínicas de Porto Alegre (HCPA) #14-0544. All effort has been made to minimize the animals' suffering or discomfort and to use the minimum number of animals necessary to obtain reliable results.

PEER REVIEW

The peer review history for this article is available at https://publons.com/publon/10.1002/jnr.24980.

DATA AVAILABILITY STATEMENT

The data that support the findings of this study are available from the corresponding author upon reasonable request.

ORCID

Letícia Barbieri Caus https://orcid.org/0000-0001-5698-8693
Mayara Vendramin Pasquetti https://orcid.org/0000-0002-7186-2877
Bianca Seminotti https://orcid.org/0000-0002-9803-7746
Michael Woontner https://orcid.org/0000-0002-9940-291X
Moacir Wajner https://orcid.org/0000-0001-6372-1807
Maria Elisa Calcagnotto https://orcid.org/0000-0001-8196-0596

REFERENCES

Amaral, A. U., Seminotti, B., da Silva, J. C., de Oliveira, F. H., Ribeiro, R. T., Leipnitz, G., Souza, D. O., & Wajner, M. (2019). Acute lysine overload provokes marked striatum injury involving oxidative stress signaling pathways in glutaryl-CoA dehydrogenase deficient mice. *Neurochemistry International*, *129*, 104467. https://doi.org/10.1016/j.neuint.2019.104467

Amaral, A. U., Seminotti, B., da Silva, J. C., de Oliveira, F. H., Ribeiro, R. T., Vargas, C. R., Leipnitz, G., Santamaría, A., Souza, D. O., & Wajner, M. (2018). Induction of neuroinflammatory response and histopathological alterations caused by quinolinic acid administration in the striatum of glutaryl-CoA dehydrogenase deficient mice. *Neurotoxicity Research*, *33*, 593–606. https://doi.org/10.1007/s12640-017-9848-0

Beal, M. F., Kowall, N. W., Ellison, D. W., Mazurek, M. F., Swartz, K. J., & Martin, J. B. (1986). Replication of the neurochemical characteristics of Huntington's disease by quinolinic acid. *Nature*, *321*, 168–171. https://doi.org/10.1038/321168a0

Bosman, D. K., Deutz, N. E. P., De Graaf, A. A., Vd Hulst, R. W. N., Van Eijk, H. M. H., Bovée, W. M. M. J., Maas, M. A. W., Jörning, G. G. A., & Chamuleau, R. A. F. M. (1990). Changes in brain metabolism during hyperammonemia and acute liver failure: Results of a comparative 1H-NMR spectroscopy and biochemical investigation. *Hepatology*, *12*, 281–290. https://doi.org/10.1002/hep.1840120215

Boy, N., Mengler, K., Heringer-Seifert, J., Hoffmann, G. F., Garbade, S. F., & Kölker, S. (2021). Impact of newborn screening and quality of therapy on the neurological outcome in glutaric aciduria type 1: A meta-analysis. *Genetics in Medicine*, *23*, 13–21. https://doi.org/10.1038/s41436-020-00971-4

Brickell, K., Nicholson, L. F., Waldvogel, H., & Faull, R. L. (1999). Chemical and anatomical changes in the striatum and substantia nigra following quinolinic acid lesions in the striatum of the rat: A detailed time course of the cellular and GABAA receptor changes. *Journal of Chemical Neuroanatomy*, *17*, 75–97. https://doi.org/10.1016/S0891-0618(99)00029-0

Buzsáki, G. (Ed.) (2006). The gamma buzz: Gluing by oscillations in the waking brain. *Rhythms of the brain* (pp. 231–261). New York, NY: Oxford University Press, Inc. https://doi.org/10.1093/acprof:oso/9780195301069.001.0001

Buzsáki, G., & Wang, X.-J. (2012). Mechanisms of gamma oscillations. *Annual Review of Neuroscience*, *35*, 203–225. https://doi.org/10.1146/annurev-neuro-062111-150444

Cerisola, A., Campistol, J., Pérez-Dueñas, B., Poo, P., Pineda, M., García-Cazorla, A., Sanmartí, F. X., Ribes, A., & Vilaseca, M. A. (2009). Seizures versus dystonia in encephalopathic crisis of glutaric aciduria type I. *Pediatric Neurology*, *40*, 426–431. https://doi.org/10.1016/j.pediatrneurol.2008.12.009

Colín-González, A. L., Paz-Loyola, A. L., Serratos, I., Seminotti, B., Ribeiro, C. A. J., Leipnitz, G., Souza, D. O., Wajner, M., & Santamaría, A. (2015). Toxic synergism between quinolinic acid and organic acids accumulating in glutaric acidemia type I and in disorders of propionate metabolism in rat brain synaptosomes: Relevance for metabolic acidemias. *Neuroscience*, *308*, 64–74. https://doi.org/10.1016/j.neuroscience.2015.09.002

de Oliveira, D. L., Horn, J. F., Rodrigues, J. M., Frizzo, M. E., Moriguchi, E., Souza, D. O., & Wofchuk, S. (2004). Quinolinic acid promotes seizures and decreases glutamate uptake in young rats: Reversal by orally administered guanosine. *Brain Research*, *1018*, 48–54. https://doi.org/10.1016/j.brainres.2004.05.033

Feng, Q., Ma, Y., Mu, S., Wu, J., Chen, S., OuYang, L., & Lei, W. (2014). Specific reactions of different striatal neuron types in morphology induced by quinolinic acid in rats. *PLoS ONE*, *9*, e91512. https://doi.org/10.1371/journal.pone.0091512

Goodman, S. I. (2004). Development of pathogenic concepts in glutaryl-CoA dehydrogenase deficiency: The challenge. *Journal of Inherited Metabolic Disease*, *27*, 801–803. https://doi.org/10.1023/B:BOLI.0000045761.01465.47

Goodman, S. I., Markey, S. P., Moe, P. G., Miles, B. S., & Teng, C. C. (1975). Glutaric aciduria; A "new" disorder of amino acid metabolism. *Biochemical Medicine*, *12*, 12–21. https://doi.org/10.1016/0006-2944(75)90091-5

Heyes, M. P. (1987). Hypothesis: A role for quinolinic acid in the neuropathology of glutaric aciduria type I. *Canadian Journal of Neurological Sciences*, *14*, 441–443. https://doi.org/10.1017/S0317167100037872

Hübel, N., & Ullah, G. (2016). Anions govern cell volume: A case study of relative astrocytic and neuronal swelling in spreading depolarization. *PLoS ONE*, *11*, e0147060. https://doi.org/10.1371/journal.pone.0147060

Koeller, D. M., Woontner, M., Crnic, L. S., Kleinschmidt-DeMasters, B., Stephens, J., Hunt, E. L., & Goodman, S. I. (2002). Biochemical, pathologic and behavioral analysis of a mouse model of glutaric acidemia type I. *Human Molecular Genetics*, *11*, 347–357. https://doi.org/10.1093/hmg/11.4.347

Kölker, S., Christensen, E., Leonard, J. V., Greenberg, C. R., Boneh, A., Burlina, A. B., Burlina, A. P., Dixon, M., Duran, M., García Cazorla, A., Goodman, S. I., Koeller, D. M., Kyllerman, M., Mühlhausen, C., Müller, E., Okun, J. G., Wilcken, B., Hoffmann, G. F., & Burgard, P. (2011). Diagnosis and management of glutaric aciduria type I—Revised recommendations. *Journal of Inherited Metabolic Disease*, *34*, 677–694. https://doi.org/10.1007/s10545-011-9289-5

La Cruz, V.- P.-D., Carrillo-Mora, P., & Santamaría, A. (2012). Quinolinic acid, an endogenous molecule combining excitotoxicity, oxidative stress and other toxic mechanisms. *International Journal of Tryptophan Research*, *5*, IJTR.S8158. https://doi.org/10.4137/IJTR.S8158

Lasztóczi, B., & Klausberger, T. (2014). Layer-specific GABAergic control of distinct gamma oscillations in the CA1 hippocampus. *Neuron*, *81*, 1126–1139. https://doi.org/10.1016/j.neuron.2014.01.021

Lindner, M., Kölker, S., Schulze, A., Christensen, E., Greenberg, C. R., & Hoffmann, G. F. (2004). Neonatal screening for glutaryl-CoA dehydrogenase deficiency. *Journal of Inherited Metabolic Disease*, *27*, 851–859. https://doi.org/10.1023/B:BOLI.0000045769.96657.af

Maddison, D. C., & Giorgini, F. (2015). The kynurenine pathway and neurodegenerative disease. *Seminars in Cell & Developmental Biology*, *40*, 134–141. https://doi.org/10.1016/j.semcdb.2015.03.002

Masuki, S., & Nose, H. (2009). Increased cerebral activity suppresses baroreflex control of heart rate in freely moving mice. *Journal of Physiology*, *587*, 5783–5794. https://doi.org/10.1113/jphysiol.2009.176164

McClelland, V. M., Bakalinova, D. B., Hendriksz, C., & Singh, R. P. (2009). Glutaric aciduria type 1 presenting with epilepsy. *Developmental Medicine and Child Neurology*, *51*, 235–239. https://doi.org/10.1111/j.1469-8749.2008.03240.x

Panthi, S., & Leitch, B. (2019). The impact of silencing feed-forward parvalbumin-expressing inhibitory interneurons in the cortico-thalamocortical network on seizure generation and behaviour. *Neurobiology of Diseases*, *132*, 104610. https://doi.org/10.1016/j.nbd.2019.104610

Paxinos, G., & Franklin, K. B. J. (2001). *The mouse brain in stereotaxic coordinates* (2th ed.). San Diego, CA: Academic Press.

Percie du Sert, N., Hurst, V., Ahluwalia, A., Alam, S., Avey, M. T., Baker, M., Browne, W. J., Clark, A., Cuthill, I. C., Dirnagl, U., Emerson, M., Garner, P., Holgate, S. T., Howells, D. W., Karp, N. A., Lazic, S. E., Lidster, K., MacCallum, C. J., Macleod, M., … Würbel, H. (2020). The ARRIVE guidelines 2.0: Updated guidelines for reporting animal research. *PLoS Biology*, *18*, e3000410. https://doi.org/10.1371/journal.pbio.3000410

Pierozan, P., Gonçalves Fernandes, C., Ferreira, F., & Pessoa-Pureur, R. (2014). Acute intrastriatal injection of quinolinic acid provokes long-lasting misregulation of the cytoskeleton in the striatum, cerebral cortex and hippocampus of young rats. *Brain Research*, *1577*, 1–10. https://doi.org/10.1016/j.brainres.2014.06.024

Racine, R. J. (1972). Modification of seizure activity by electrical stimulation: II. Motor seizure. *Electroencephalography and Clinical Neurophysiology*, *32*, 281–294. https://doi.org/10.1016/0013-4694(72)90177-0

Reynolds, N. C., Lin, W., Meyer Cameron, C., & Roerig, D. L. (1997). Differential responses of extracellular GABA to intrastriatal perfusions of 3-nitropropionic acid and quinolinic acid in the rat. *Brain Research*, *778*, 140–149. https://doi.org/10.1016/S0006-8993(97)01048-2

Robinson, N. (1969). Histochemical changes in neocortex and corpus callosum after intracranial injection. *Journal of Neurology, Neurosurgery and Psychiatry*, *32*, 317–323. https://doi.org/10.1136/jnnp.32.4.317

Sabel, B. A., Labbe, R., & Stein, D. G. (1985). The saline effect: Minimizing the severity of brain damage by reduction of secondary degeneration. *Experimental Neurology*, *88*, 95–107. https://doi.org/10.1016/0014-4886(85)90116-5

Schwarcz, R., Brush, G. S., Foster, A. C., & French, E. D. (1984). Seizure activity and lesions after intrahippocampal quinolinic acid injection. *Experimental Neurology*, *84*, 1–17. https://doi.org/10.1016/0014-4886(84)90001-3

Seminotti, B., Amaral, A. U., Ribeiro, R. T., Rodrigues, M. D. N., Colín-González, A. L., Leipnitz, G., Santamaría, A., & Wajner, M. (2016). Oxidative stress, disrupted energy metabolism, and altered

signaling pathways in glutaryl-CoA dehydrogenase knockout mice: Potential implications of quinolinic acid toxicity in the neuropathology of glutaric acidemia type I. *Molecular Neurobiology*, *53*, 6459–6475. https://doi.org/10.1007/s12035-015-9548-9

Sitta, A., Guerreiro, G., de Moura Coelho, D., da Rocha, V. V., dos Reis, B. G., Sousa, C., Vilarinho, L., Wajner, M., & Vargas, C. R. (2021). Clinical, biochemical and molecular findings of 24 Brazilian patients with glutaric acidemia type 1: 4 novel mutations in the GCDH gene. *Metabolic Brain Disease*, *36*, 205–212. https://doi.org/10.1007/s11011-020-00632-0

Stigsby, B., Yarworth, S. M., Rahbeeni, Z., Dabbagh, O., de Gier Munk, C., Abdo, N., Brismar, J., Gascon, G. G., & Ozand, P. T. (1994). Neurophysiologic correlates of organic acidemias: A survey of 107 patients. *Brain and Development*, *16*, 125–144. https://doi.org/10.1016/0387-7604(94)90104-X

Tort, A. B. L., Kramer, M. A., Thorn, C., Gibson, D. J., Kubota, Y., Graybiel, A. M., & Kopell, N. J. (2008). Dynamic cross-frequency couplings of local field potential oscillations in rat striatum and hippocampus during performance of a T-maze task. *Proceedings of the National Academy of Sciences of the United States of America*, *105*, 20517–20522. https://doi.org/10.1073/pnas.0810524105

Trinka, E., Cock, H., Hesdorffer, D., Rossetti, A. O., Scheffer, I. E., Shinnar, S., Shorvon, S., & Lowenstein, D. H. (2015). A definition and classification of status epilepticus—Report of the ILAE Task Force on Classification of Status Epilepticus. *Epilepsia*, *56*, 1515–1523. https://doi.org/10.1111/epi.13121

Ullah, G., Wei, Y., Dahlem, M. A., Wechselberger, M., & Schiff, S. J. (2015). The role of cell volume in the dynamics of seizure, spreading depression, and anoxic depolarization. *PLoS Computational Biology*, *11*, e1004414. https://doi.org/10.1371/journal.pcbi.1004414

van der Meer, M. A. A. (2009). Low and high gamma oscillations in rat ventral striatum have distinct relationships to behavior, reward, and spiking activity on a learned spatial decision task. *Frontiers in Integrative Neuroscience*, *3*, 9. https://doi.org/10.3389/neuro.07.009.2009

Varadkar, S., & Surtees, R. A. H. (2004). Glutaric aciduria type I and kynurenine pathway metabolites: A modified hypothesis. *Journal of Inherited Metabolic Disease*, *27*, 835–842. https://doi.org/10.1023/B:BOLI.0000045767.42193.97

Vendramin Pasquetti, M., Meier, L., Loureiro, S., Ganzella, M., Junges, B., Barbieri Caus, L., Umpierrez Amaral, A., Koeller, D. M., Goodman, S., Woontner, M., Gomes de Souza, D. O., Wajner, M., & Calcagnotto, M. E. (2017). Impairment of GABAergic system contributes to epileptogenesis in glutaric acidemia type I. *Epilepsia*, *58*, 1771–1781. https://doi.org/10.1111/epi.13862

Vogels, B. A., Maas, M. A., Daalhuisen, J., Quack, G., & Chamuleau, R. A. (1997). Memantine, a noncompetitive NMDA receptor antagonist improves hyperammonemia-induced encephalopathy and acute hepatic encephalopathy in rats. *Hepatology*, *25*, 820–827. https://doi.org/10.1002/hep.510250406

Wajner, M. (2019). Neurological manifestations of organic acidurias. *Nature Reviews. Neurology*, *15*, 253–271. https://doi.org/10.1038/s41582-019-0161-9

Wilson, C. S., & Mongin, A. A. (2018). Cell volume control in healthy brain and neuropathologies. *Current Topics in Membranes*, *81*, 385–455. https://doi.org/10.1016/bs.ctm.2018.07.006

Yaksh, T. L., Jang, J., Nishiuchi, Y., Braun, K. P., Ro, S., & Goodman, M. (1991). The utility of 2-hydroxypropyl-β-cyclodextrin as a vehicle for the intracerebral and intrathecal administration of drugs. *Life Sciences*, *48*, 623–633. https://doi.org/10.1016/0024-3205(91)90537-L

Yalnizoğlu, D., Sari, N., Turanli, G., Coşkun, T., & Topçu, M. (2005). Neurophysiologic features in glutaric aciduria type I. *Turkish Journal of Pediatrics*, *47*, 153–158.

Zinnanti, W. J., Lazovic, J., Wolpert, E. B., Antonetti, D. A., Smith, M. B., Connor, J. R., Woontner, M., Goodman, S. I., & Cheng, K. C. (2006). A diet-induced mouse model for glutaric aciduria type I. *Brain*, *129*, 899–910. https://doi.org/10.1093/brain/awl009

SUPPORTING INFORMATION

Additional supporting information may be found in the online version of the article at the publisher's website.

FIGURE S1 Changes in the power of different brain oscillations over time for all groups. (a) The power of delta increased at P34 in relation to: (a) P32/0 for all QA groups and $Gcdh^{-/-}$-N-V animals ($Gcdh^{-/-}$-Lys-QA: $p = 0.009$; $Gcdh^{+/+}$-Lys-QA: $p < 0.001$; $Gcdh^{-/-}$-N-QA: $p < 0.001$; $Gcdh^{-/-}$-N-V: $p = 0.003$); (b) P32/15 for $Gcdh^{-/-}$-Lys-QA ($p = 0.03$) and $Gcdh^{+/+}$-Lys-QA groups ($p = 0.003$). No differences over time were found for $Gcdh^{-/-}$-Lys-V ($p = 0.20$) and $Gcdh^{+/+}$-Lys-V animals ($p = 0.12$). (b) Power values of theta increased at P34 in relation to: (a) P32/0 in all groups, except $Gcdh^{-/-}$-Lys-V ($Gcdh^{-/-}$-Lys-QA: $p = 0.03$; $Gcdh^{+/+}$-Lys-QA: $p < 0.001$; $Gcdh^{-/-}$-N-QA: $p < 0.001$; $Gcdh^{+/+}$-Lys-V: $p = 0.005$; $Gcdh^{-/-}$-N-V: $p = 0.01$); (b) P32/15 in QA groups ($Gcdh^{-/-}$-Lys-QA: $p = 0.003$; $Gcdh^{+/+}$-Lys-QA: $p = 0.001$; and $Gcdh^{-/-}$-N-QA: $p = 0.005$). Power values of theta increased at P32/45 in relation to P32/0 in all groups, except $Gcdh^{-/-}$-Lys groups ($Gcdh^{+/+}$-Lys-QA: $p = 0.03$; $Gcdh^{-/-}$-N-QA: $p = 0.009$; $Gcdh^{+/+}$-Lys-V: $p = 0.03$; $Gcdh^{-/-}$-N-V: $p = 0.05$). It also increased at P32/30 in relation to P32/0 and at P34 in relation to P32/30 in $Gcdh^{+/+}$-Lys-QA mice ($p = 0.03$; $p = 0.05$) and at P32/45 in relation to P32/15 in $Gcdh^{-/-}$-Lys-QA group ($p = 0.03$). No differences were found for $Gcdh^{-/-}$-Lys-V animals ($p = 0.31$). (c) The power of slow gamma increased at P34 in relation to: (a) P32/0 in all groups ($Gcdh^{-/-}$-Lys-QA: $p = 0.02$; $Gcdh^{+/+}$-Lys-QA: $p < 0.001$; $Gcdh^{-/-}$-N-QA: $p < 0.001$; $Gcdh^{-/-}$-Lys-V: $p = 0.001$; $Gcdh^{+/+}$-Lys-V: $p < 0.001$; $Gcdh^{-/-}$-N-V: $p < 0.001$); and (b) P32/15 in all groups, except $Gcdh^{-/-}$-Lys-V ($Gcdh^{-/-}$-Lys-QA: $p = 0.001$; $Gcdh^{+/+}$-Lys-QA: $p < 0.001$; $Gcdh^{-/-}$-N-QA: $p = 0.005$; $Gcdh^{+/+}$-Lys-V: $p = 0.005$; $Gcdh^{-/-}$-N-V: $p = 0.003$). The power of slow gamma increased at P32/45 in relation to: (a) P32/0 in $Gcdh^{+/+}$-Lys-QA ($p = 0.002$), $Gcdh^{-/-}$-N-QA ($p = 0.04$), and $Gcdh^{+/+}$-Lys-V animals ($p = 0.008$); and (b) P32/15 in $Gcdh^{-/-}$-Lys-QA ($p = 0.03$) and $Gcdh^{+/+}$-Lys-QA animals ($p = 0.05$). It also increased at P32/30 in relation to P32/0 in $Gcdh^{+/+}$-Lys-QA ($p = 0.05$), $Gcdh^{+/+}$-Lys-V ($p = 0.001$), and $Gcdh^{-/-}$-N-V animals ($p = 0.05$). (d) The power of middle gamma increased at P34 in relation to: (a) P32/0 in all groups ($Gcdh^{-/-}$-Lys-QA: $p = 0.03$; $Gcdh^{+/+}$-Lys-QA: $p < 0.001$; $Gcdh^{-/-}$-N-QA: $p < 0.001$; $Gcdh^{-/-}$-Lys-V: $p = 0.003$; $Gcdh^{+/+}$-Lys-V: $p < 0.001$; $Gcdh^{-/-}$-N-V: $p = 0.05$); (b) P32/15 in all groups, except $Gcdh^{-/-}$-Lys-V ($Gcdh^{-/-}$-Lys-QA: $p = 0.004$; $Gcdh^{+/+}$-Lys-QA: $p < 0.001$; $Gcdh^{-/-}$-N-QA: $p = 0.001$; $Gcdh^{-/-}$-N-V: $p < 0.001$; $Gcdh^{+/+}$-Lys-V: $p < 0.001$); (c) P32/30 in $Gcdh^{-/-}$-Lys-V mice ($p = 0.004$); P32/45 in $Gcdh^{-/-}$-Lys-V ($p = 0.03$), $Gcdh^{-/-}$-N-V ($p = 0.01$), and $Gcdh^{+/+}$-Lys-V animals ($p = 0.04$). It increased at P32/45 in relation to: (a) P32/0 in $Gcdh^{-/-}$-N-QA ($p = 0.03$), $Gcdh^{+/+}$-Lys-QA ($p = 0.001$), and $Gcdh^{+/+}$-Lys-V animals ($p = 0.04$); and b) P32/15 in $Gcdh^{+/+}$-Lys-QA animals ($p = 0.03$). It also increased at P32/30 in relation to P32/0 in $Gcdh^{+/+}$-Lys-QA ($p = 0.02$) and $Gcdh^{+/+}$-Lys-V animals ($p = 0.02$). (e) The power of fast gamma increased at P34 in relation to: (a) P32/0 in all groups ($Gcdh^{-/-}$-Lys-QA: $p = 0.03$; $Gcdh^{+/+}$-Lys-QA: $p < 0.001$; $Gcdh^{-/-}$-N-QA: $p < 0.001$; $Gcdh^{-/-}$-Lys-V: $p = 0.01$; $Gcdh^{-/-}$-N-V: $p < 0.001$; $Gcdh^{+/+}$-Lys-V: $p < 0.001$); b) P32/15 in all groups, except $Gcdh^{-/-}$-Lys-V ($Gcdh^{-/-}$-Lys-QA: $p = 0.01$; $Gcdh^{+/+}$-Lys-QA: $p < 0.001$; $Gcdh^{-/-}$-N-QA: $p = 0.01$; $Gcdh^{-/-}$-N-V: $p = 0.01$; $Gcdh^{+/+}$-Lys-V: $p = 0.005$); c) P32/45

in *Gcdh*$^{-/-}$-Lys-V ($p = 0.01$) and *Gcdh*$^{+/+}$-Lys-V mice ($p = 0.02$); and d) P32/30 in*Gcdh*$^{+/+}$-Lys-V mice ($p = 0.04$). It also increased at P32/45 in relation to P32/0 in *Gcdh*$^{-/-}$-N-QA animals ($p = 0.04$). Values and statistical significance are described on Table S2

FIGURE S2 Changes in left index (a) and theta/delta ratio (b) over time for all groups. (a) Note that at P32/0 left index values increased in relation to baseline in *Gcdh*$^{-/-}$-Lys-QA ($p = 0.01$), *Gcdh*$^{-/-}$-Lys-V ($p = 0.03$), and *Gcdh*$^{+/+}$-Lys-QA mice ($p = 0.05$). At P32/15, values remained increased only for *Gcdh*$^{-/-}$-Lys-QA animals ($p = 0.003$). At P34, left index decreased in relation to: (a) P32/0 in *Gcdh*$^{+/+}$-Lys-QA ($p = 0.03$), *Gcdh*$^{+/+}$-Lys-QA ($p < 0.001$), and *Gcdh*$^{-/-}$-N-QA animals ($p = 0.02$); and b) P32/15 for *Gcdh*$^{-/-}$-Lys-QA ($p = 0.008$) and *Gcdh*$^{+/+}$-Lys-QA animals ($p = 0.03$). Only *Gcdh*$^{+/+}$-Lys-V mice had decreased left index at P32/15 and P32/30 in relation to P32/0 ($p = 0.03$ and $p < 0.001$, respectively), while both *Gcdh*$^{+/+}$-Lys-V and *Gcdh*$^{+/+}$-Lys-QA had decreased left index values at P32/45 in relation to P32/0 ($p < 0.001$ and $p = 0.004$, respectively). No differences were found for *Gcdh*$^{-/-}$-N-V mice. (b) Note that, at P32/0, *Gcdh*$^{-/-}$-Lys-QA, *Gcdh*$^{+/+}$-Lys-QA, *Gcdh*$^{-/-}$-N-QA, and *Gcdh*$^{+/+}$-Lys-V groups had decreased values of theta/delta ratio in relation to baseline ($p = 0.008$, $p = 0.004$, $p = 0.013$, and $p = 0.004$, respectively). At P32/15, theta/delta ratio decreased in relation to baseline in *Gcdh*$^{-/-}$-Lys-QA ($p = 0.001$) and *Gcdh*$^{-/-}$-N-QA animals ($p = 0.02$). At P32/30, P32/45, and P34 theta/delta ratio increased in relation to P32/0 in *Gcdh*$^{+/+}$-Lys groups (*Gcdh*$^{+/+}$-Lys-QA: $p = 0.02$, $p = 0.01$, and $p < 0.001$, respectively; *Gcdh*$^{+/+}$-Lys-V: $p = 0.007$, $p = 0.001$ and $p < 0.001$, respectively). At P32/45, the ratio increased in relation to P32/15 in *Gcdh*$^{-/-}$-Lys-QA animals ($p = 0.01$) and in relation to baseline and P32/0 in *Gcdh*$^{-/-}$-N-V group ($p = 0.04$). At P34, the ratio increased in relation to P32/15 in *Gcdh*$^{-/-}$-Lys-QA ($p = 0.008$) and *Gcdh*$^{-/-}$-N-QA animals ($p = 0.005$) and also in relation to P32/0 for *Gcdh*$^{-/-}$-N-QA group ($p = 0.003$). No differences were found for *Gcdh*$^{-/-}$-Lys-V animals ($p = 0.27$). Values and statistical significances are described on Table S3

TABLE S1 Sex comparison for every analysis performed

TABLE S2 Power ratio of brain oscillations at different time-periods

TABLE S3 Left index and theta/delta ratio at different time-periods

Transparent Peer Review Report

Transparent Science Questionnaire for Authors

How to cite this article: Barbieri Caus, L., Pasquetti, M. V., Seminotti, B., Woontner, M., Wajner, M., & Calcagnotto, M. E. (2022). Increased susceptibility to quinolinic acid-induced seizures and long-term changes in brain oscillations in an animal model of glutaric acidemia type I. *Journal of Neuroscience Research*, 100, 992–1007. https://doi.org/10.1002/jnr.24980